AIP Advances

Tuning of colossal dielectric constant in gold-polypyrrole composite nanotubes using in-situ x-ray diffraction techniques

Abhisakh Sarma and Milan K. Sanyal

Citation: AIP Advances **4**, 097121 (2014); doi: 10.1063/1.4896122
View online: http://dx.doi.org/10.1063/1.4896122
View Table of Contents: http://scitation.aip.org/content/aip/journal/adva/4/9?ver=pdfcov
Published by the AIP Publishing

AIP ADVANCES **4**, 097121 (2014)

Tuning of colossal dielectric constant in gold-polypyrrole composite nanotubes using in-situ x-ray diffraction techniques

Abhisakh Sarma and Milan K. Sanyal[a]
Saha Institute of Nuclear Physics, 1/AF Bidhannagar, Kolkata 700 064, India

(Received 6 March 2014; accepted 8 September 2014; published online 17 September 2014)

In-situ x-ray diffraction technique has been used to study the growth process of gold incorporated polypyrrole nanotubes that exhibit colossal dielectric constant due to existence of quasi-one-dimensional charge density wave state. These composite nanotubes were formed within nanopores of a polycarbonate membrane by flowing pyrrole monomer from one side and mixture of ferric chloride and chloroauric acid from other side in a sample cell that allows collection of x-ray data during the reaction. The size of the gold nanoparticle embedded in the walls of the nanotubes was found to be dependent on chloroauric acid concentration for nanowires having diameter more than 100 nm. For lower diameter nanotubes the nanoparticle size become independent of chloroauric acid concentration and depends on the diameter of nanotubes only. The result of this study also shows that for 50 nm gold-polypyrrole composite nanotubes obtained with 5.3 mM chloroauric acid gives colossal dielectric constant of about 10^7. This value remain almost constant over a frequency range from 1Hz to 10^6 Hz even at 80 K temperature. [http://dx.doi.org/10.1063/1.4896122]

I. INTRODUCTION

In recent years enormous amount of academic research have been carried out in the general areas of flexible nanodielectric materials (FNDMs), primarily composed of polymer matrix with embedded nanoparticles, to develop compact capacitors and energy storage devices.[1,2] Similar applicable composite nanomaterials are also being developed for several other applications, like carbon nanotube polymer nanocomposites for getting high thermoelectric figure of merit,[3] dendrimer-metal nanocomposites to obtain enhanced third-order nonlinear optical properties,[4] magnetic nanoparticles embedded in polymer matrices for potential application in electromagnetic interference shielding,[5] polyaniline nanofibers decorated with gold nanoparticles[6,7] for nonvolatile memory devices[8] etc.

Development of FNDMs to tune effective dielectric constant (ε_{eff}) of a polymer ($\varepsilon_1 \approx 3$) by introducing inorganic nano fillers having higher dielectric constant ($\varepsilon_2 \approx 100$) with volume fraction of ϕ, is of prime importance to achieve flexible and compact energy storage capacitorss[9] particularly using metal-polymer composites,[10] where ε_{eff} can be written as, $(1-\phi)\varepsilon_1 + \phi\varepsilon_2$. It is interesting to note that the effective dielectric constant [$\varepsilon_{eff} = \varepsilon_1(1-\phi/\phi_c)^{-s}$ with $s > 0$] of a metal-polymer composite can exhibit much higher value ($\varepsilon_{eff} \approx 1000$) compared to ε_1 and ε_2 as the volume fraction of ϕ approaches the percolation threshold (ϕ_c), defined as the critical volume fraction at which embedded metal nanoparticles establishes a conducting channel across the sample. One very important aspect in this rapidly developing field of research is to get a low value of ϕ_c so that obtained FNDMs remains flexible.[10] It is essential to develop an understanding of the microstructure of the metal-polymer composite to obtain high dielectric constant. One can also get colossal dielectric

[a]Electronic mail: milank.sanyal@saha.ac.in

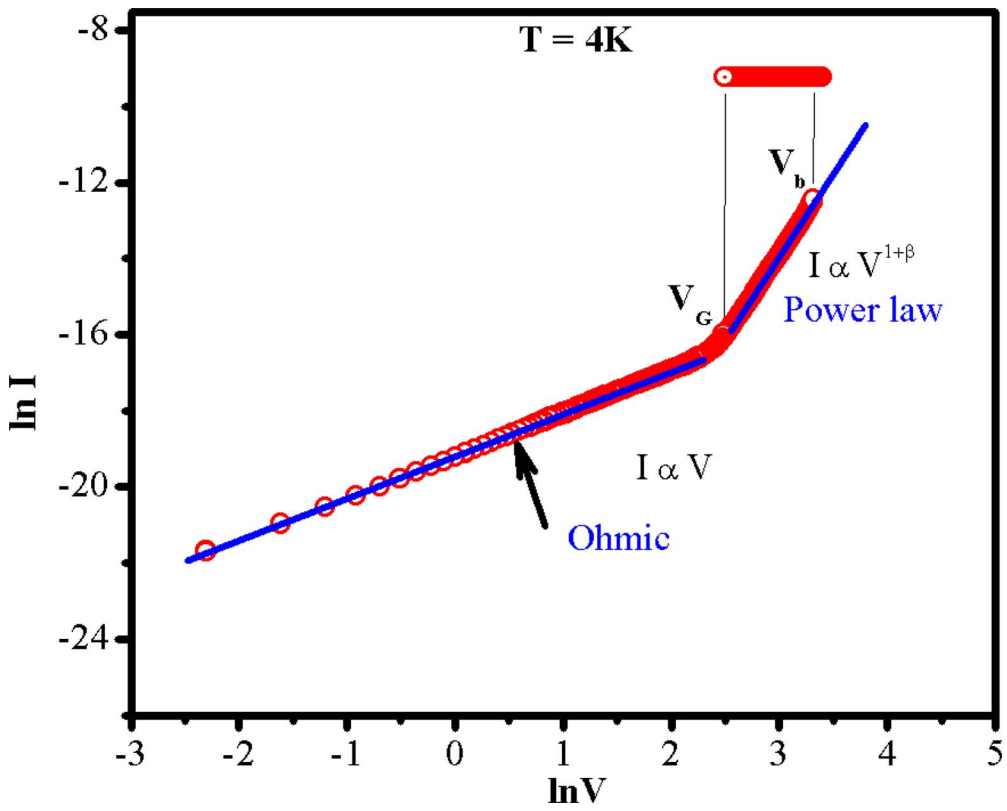

FIG. 1. Current-Voltage characteristics of gold-polypyrrole composite nanotube.

constant ε of the order of 10^5 in materials like $CoCuTi_4O_{12}$ (CCTO) and $La_{2-x}Sr_xNiO_2$ (LSMO) due to exitance of charge ordered state[11] and in several other materials that exhibit charge density wave (CDW) state.[12–15] It is well known[12,16–18] that above certain threshold electric field (E_b) these CDW materials goes through a switching transition that enhances the conductivity of the system significantly. Below this E_b, weakly pinned[15] CDW state exhibit colossal dielectric constant[13,14] but the dielectric loss increases in these CDW systems as E_b is approached. But incorporation of these materials in flexible polymer matrix has not been achieved till date.

It has been shown recently that quasi-one dimensional (1D) CDW state can exist in nanotubes of polypyrrole[16–18] and by incorporating gold nanoparticles with very little volume fraction (< 1 %) in polypyrrole nanotubes, the quasi 1D CDW state of these nanocomposite nanotubes can be extended beyond liquid nitrogen temperature.[19,20] All the characteristics of CDW systems are observed in these polymer nanotubes, like power-law behavior ($I \propto V^{1+\beta}$) with the exponent $1 + \beta > 3$ in current-voltage plots below E_b and above E_b these nanotubes exhibit negative differential resistance and noise enhancement in the reversible switched state.[16,17] Here we have shown that by tuning the size and volume fraction of gold nano-particles, colossal dielectric constant can be obtained in these composite nanotubes. These gold-polypyrrole composite nanotubes may be used for various technological applications at liquid nitrogen temperature. Particularly these FNDMs may be useful as capacitor materials working around 1 MHz range.[21]

One typical I-V curve of 0.4 wt% gold incorporated 200 nm polypyrrole nanotubes is shown in Fig. 1. From the figure it is clear that low temperature I-V characteristic of these nanotubes show three distinct zones, namely Ohmic gap zone upto voltage V_G, power law behavior zone below threshold voltage V_b (E_b) and above V_G, resistive switching above voltage V_b. In the power law zone, measured current exhibit $I \propto V^{1+\beta}$ on voltage and measured value of β was obtained in the range 3 to 9 for gold-polypyrrole nanotube.[19] These values are much higher than values obtained in

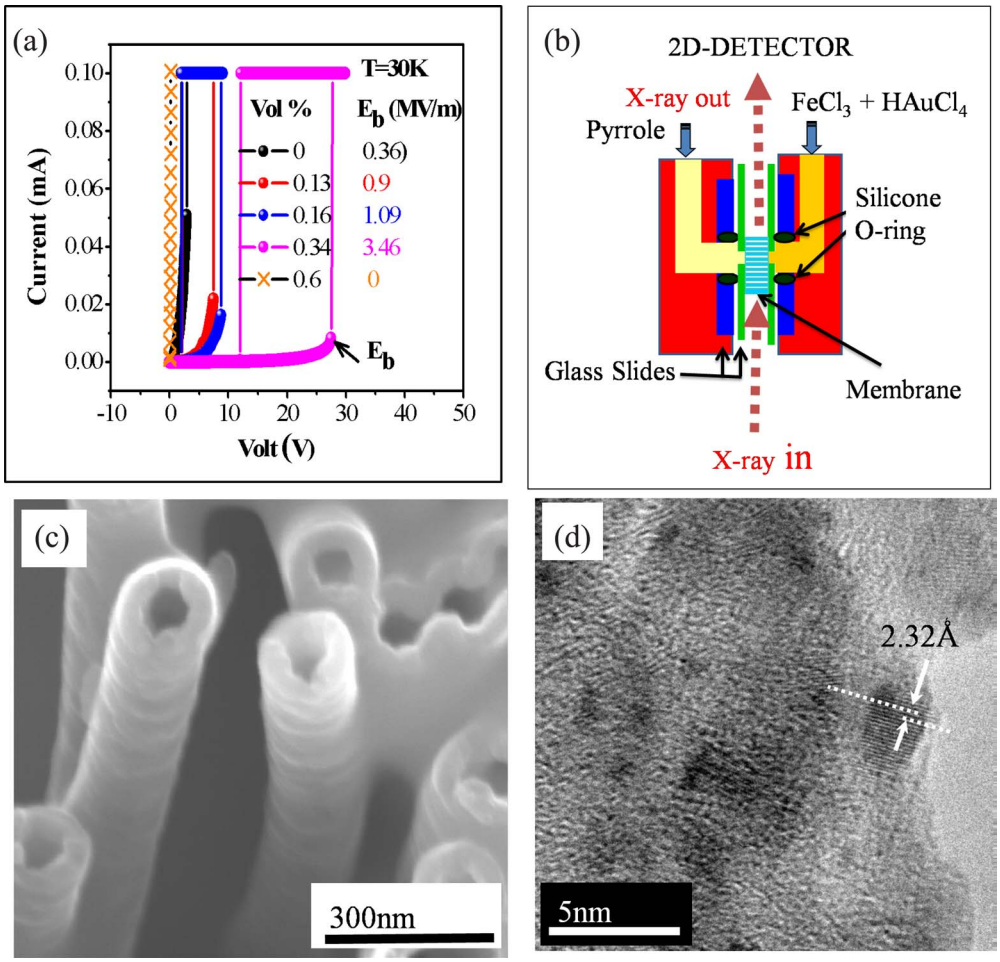

FIG. 2. (a) Electric field (E_b required to get switching transition in various polypyrrole nanowires having different volume percentage of gold, (b) The sample cell where red color corresponds to PERSPEX and blue color correspond to GLASS. Polycarbonate membrane of thickness 10 μm was placed between two centered drilled holding glasses(shown green)are used to avoid any scattering signal of gold from solution and face of membrane, (c) Scanning Electron Microscope image of gold incorporated nanotubes, the formed nanotubes were found to be monodispersed, (d)Transmission electron microscopy image, showing Au (111) crystal plane with the lattice constant of 2.07 Å

systems showing space-charge limited current (SCLC) behavior with an exponent 3/2 (Child's law) or 2 (Mott Gurney) and such high values of β can only occur in materials with CDW state.[13,14]

The obtained value of the threshold bias field E_b is found to be independent of bias polarity and the value can be tuned with the diameter of the nanowires and temperature; the threshold bias can also be tuned with intensity of photo illumination.[18] In Fig. 2(a) we have shown typical variation of switching transition characteristics of polypyrrole nanotubes having different amount of gold at 30 K temperature. The saturation of current at 0.1 mA is due to compliance setting. It is clear from the figure that the value of switching threshold field E_b that limit the applicability of these nanotubes as high dielectric materials, increase from 0.36 MV/m for pure polypyrrole nanotubes to 0.9, 1.06 and 3.46 MV/m as the gold weight percentage become 0.13, 0.14 and 0.4 respectively. The presence of gold nanoparticles provided control[20] on the doping and disorder in these composite nanotubes for enhancing the value of E_b and the temperature-range of CDW state.[19] But at 0.6 weight percentage (wt%) of gold, the system crosses critical concentration (ϕ_c) exhibiting rapid increase in current close to zero bias and the characteristics of CDW state could not be observed in such nanotubes.

X-ray scattering measurements are essential to determine the size and distribution of metal nanoparticles within polymer matrix as electron microscopy techniques may alter the actual size of

embedded nanoparticles due to electron beam induced coagulation process.[22] The result presented here clearly show that the growth process of these composite nanotubes can be probed with synchrotron x-ray diffraction (XRD) technique and with minor modification the presented techniques can be used to monitor growth of similar FNDMs.

II. EXPERIMENTAL METHOD

The sample cell used for the in-situ x-ray diffraction study and the schematic of the experimental arrangement is shown in Fig. 2(b). The cell is basically composed of two compartments. One compartment was filled with pyrrole monomer and other one was used to keep with a mixture of ferric chloride ($FeCl_3$) and chloroauric acid ($HAuCl_4$). The polycarbonate membrane was placed[19] between these two compartments and x-ray was allowed to pass only through the membrane, perpendicular with the pore direction and the diffraction data was collected using a two dimensional (2D) detector. The thickness of the polycarbonate membrane used in this study varied from 8 μm to 12 μm and the dimension of the incident x-ray (13 keV) beam was 10 μm X 8 μm. The two compartment sample cell used here was made with perspex (shown in Fig. 2(b) with red color). In order to obtain smooth surfaces we have used two center drilled (8 mm) glass slide (shown in blue color) over the perspex. The membrane was placed within another two glass slides (shown in green) having 1 mm central hole to make sure that the flatness of the sample is maintained so that the incident x-ray beam and the diffracted beam probe only the nanotubes inside the membrane. We have found that much bigger gold nanoparticles get deposited on the surface of membrane in this reaction due to the lack of confinement and the primary purpose of this special sample cell was to ensure that x-ray data is obtained only from the nanotubes within the membrane and not from the surface of the membrane. The experiment was carried out in P08 and P03 beamlines of PETRA-III Synchrotron at DESY, Germany. In this study we have used polycarbonate membrane of five different pore diameters (400 nm, 200 nm, 80 nm, 50 nm, 30 nm) (purchased from Whatman). Pyrrole monomer (purchased from Merck, Germany) was vacuum distilled and stored at 20^0C before use. Chloroauric acid (purchased from Alfa Aser) was used as gold source. Ferric chloride (purchased from Merck) was used as obtained.

In Fig. 2(c) and Fig. 2(d) we have shown typical scanning electron microscopy (SEM) and transmission electron microscopy (TEM) images of nanotubes obtained after the x-ray experiment by dissolving the polycarbonate template using chloroform. From the low and high magnification images, shown in Fig. 2(c) and Fig. 2(d) respectively, it is clear that gold-polypyrrole nanocomposites formed mono-dispersed nanotubes in the pores of the membrane and gold nano-particles get embedded in the wall of these nanotubes. In-situ x-ray measurements and subsequent dielectric measurements clearly show that dielectric constant of these nanotubes can be tuned by controlling the diameters of the nanotubes and the molar concentration of chloroauric acid and ferric chloride. We have presented here results obtained with membranes of five different pore diameters (400 nm, 200 nm, 80 nm, 50 nm and 30 nm) and two different concentrations of chloroauric acid (5.3 mM and 2.6 mM).

III. RESULTS AND DISCUSSION

The in-situ XRD experiments were carried out during growth of the nanotubes within pores of the membrane. For these measurements we first aligned the cell so that micron sized x-ray beam goes through the membrane ($\sim$ 10 μm width) perpendicular to pore direction over several millimeter and the alignment remains unchanged after pouring of chemicals in the both compartments of the sample cell for the reaction. The chemicals were introduced by remotely controlled motorized syringes and data was collected in the interval of 30 seconds for several hours. A typical XRD data of gold incorporated 200 nm nanotube formed with 5.3 mM chloroauric acid is shown in Fig. 3(a). We have analyzed XRD data using Willliamson-Hall analysis method[23] by extracting the width of each peak from Lorentzian fitting. From the $\beta Cos\theta$ vs $4Sin\theta$ plot we have found that gold particle size is 11 nm and weighted average strain is only 0.0045 % (shown in Fig. 3(b)) for a typical membrane having nanotubes of 200 nm diameter. For other diameter nanotube also we have checked that the strain

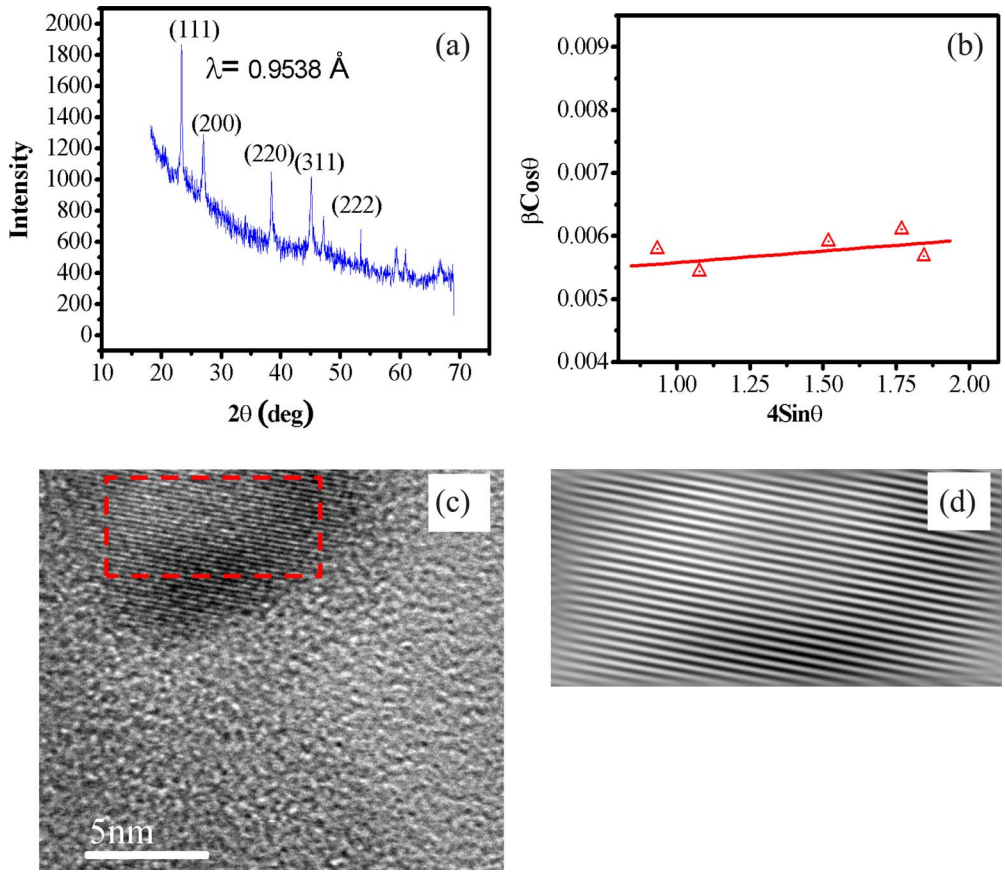

FIG. 3. (a) X-ray diffraction of the gold-incorporated 200 nm polypyrrole nanotube,(b) Williamson-Hall plot constructed from the peak profiles of the Synchrotron X-ray powder diffraction pattern, (c) TEM image of incorporated gold nanoparticle in 200 nm (5.3 mM) nanotube, (d) FFT and spatial filtered image of rectangular zone shown in (c).

is negligible. In Fig. 3(c) we have shown a typical TEM micrograph of incorporated nanoparticle. The corresponding Fast Fourier Transform (FFT) and spatially filtered image of the selected zone of the nanoparticle is shown in Fig. 3(d); these data clearly show that the micro-strain is negligible here. As a result the effect of microstrain was neglected in the determination of gold particle size from the width of the x-ray diffraction peak. The instrumental resolution for both the beamlines were extremely good and resolution width was also negligible.[24,25] In P08 and P03 beamlines the divergence of x-ray beam was 400 X 260 microrad and 150 X 80 microrad respectively. The data shown in Fig. 3(a) was collected with sample to detector distance of 100 cm and the width of Au (111) diffraction peak was 0.45^0 where contribution of beam divergence can be maximum 0.025^0. It may be noted that the measured width[26] of a typical single crystal diffraction peak at these beamlines in same configuration is 0.03^0. As the diffraction peaks of Au nanoparticles are quite broad, we reduced the sample to detector distance to 14 cm to enhance peak-to-background ratio for monitoring the chemical reaction as a function of time. At this distance Au (111) diffraction peak from nanoparticle-incorporated nanotubes appeared in typically 10 detector pixels (refer Fig. 4(b)) and we could monitor development of Au(111) diffraction peak as a function of reaction time. The details of the intensity variation of Au (111) peak is shown in Fig. 4(c). The spot in the images of two-dimensional (2D) detector (refer Fig. 4(a) and Fig. 4(b)) corresponds to Au (111) diffraction peak of the gold nanoparticle formed within the wall of 200 nm diameter nanotube (5.3 mM $HAuCl_4$ concentration). We have found that the intensity of spot increases with time and then saturates, as shown in Fig. 4(c). It is also interesting to note that the intensity of the (111) peak increases rather abruptly after about 20 minutes of reaction. We now present the results obtained from different

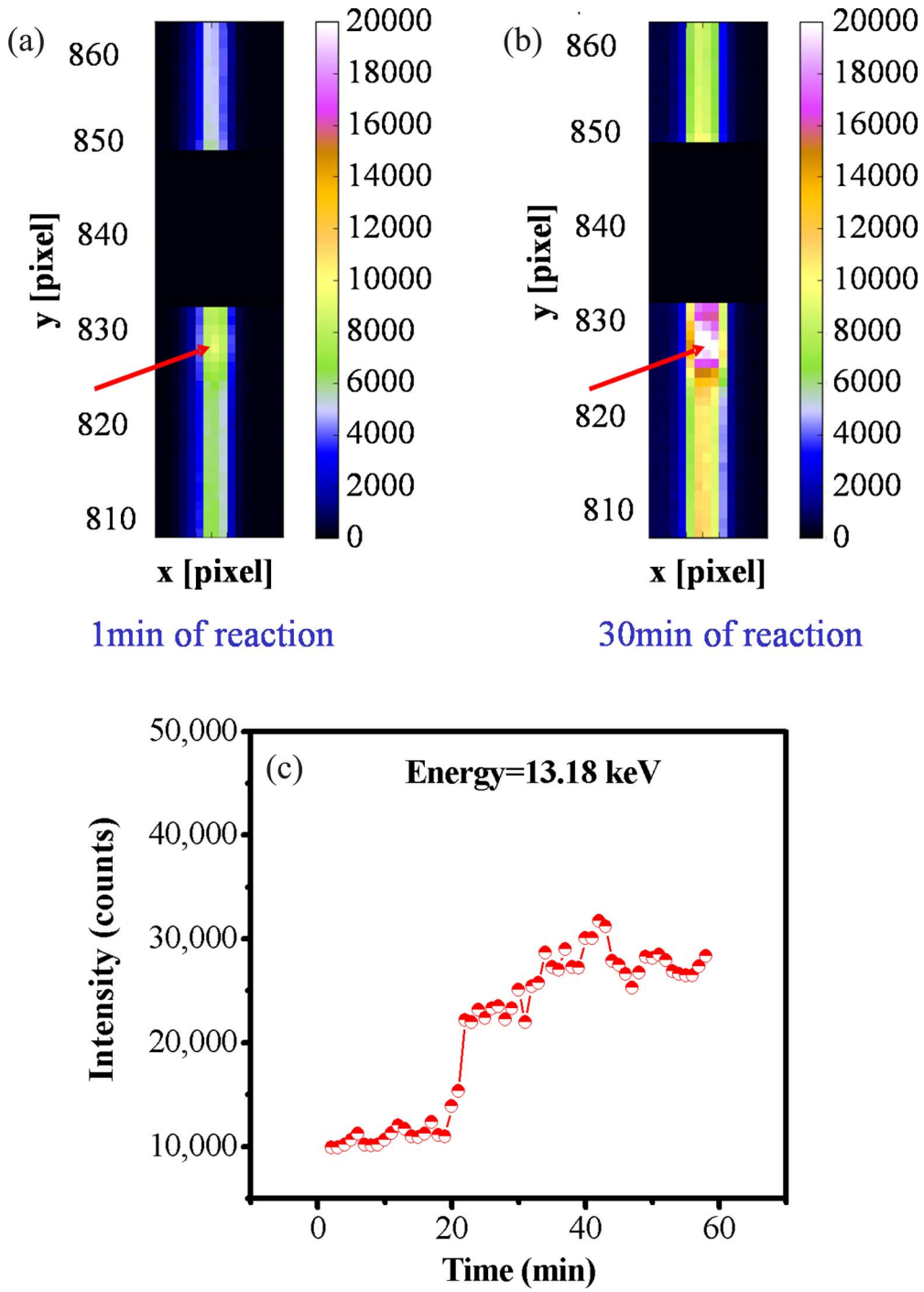

FIG. 4. XRD spot corresponding to Au (111) in 2D Pilatus detector (a) after 1min of reaction, (b) after 30 min of reaction, (c) the time evolution of the intensity of the XRD spot.

diameter nanotubes to understand the dependence of particle size on reaction time and on diameter of nanopores. In Fig. 5(a) and Fig. 5(b) we have shown, Au (111) diffraction peak of composite nanotubes having diameter of 400 nm and 80 nm respectively, after 6 min and 30 min of reaction. These data were extracted from line profile obtained from 2D image (just as shown in Fig. 4(a) and Fig. 4(b)) for 400 nm 80 nm gold incorporated nanotubes. The width of the peak obtained was 0.46^0 and 0.51^0 with 5.3 mM chloroauric acid for 400 nm and 80 nm diameter nanotubes respectively. This

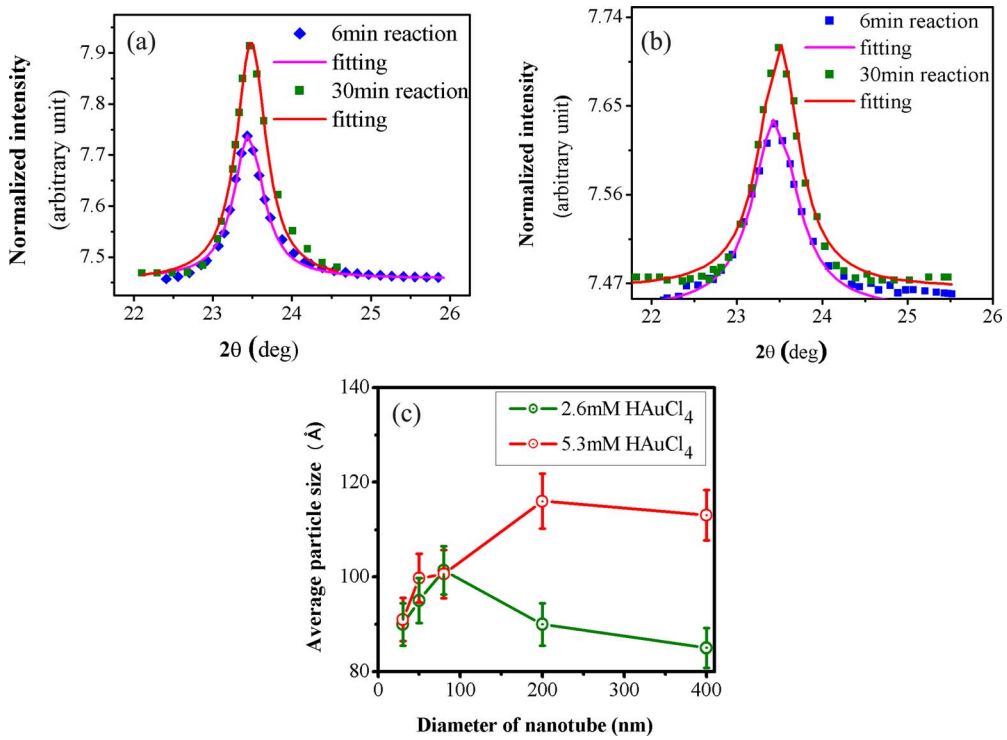

FIG. 5. The time evolution of Au (111) peak after 6 min and 30 min of reaction, (a) 400 nm nanotube, (b) 80 nm nanotube, (c) The variation of the size of incorporated gold nanoparticles with the variation of nanotube diameter for two different concentration of $HAuCl_4$. The data shown in (a) and (b) are extracted from the accumulated 2D detector image similar to the one shown in Fig. 4 for 200 nm nanotubes. The extracted counts from the detector pixels were normalized to have same background counts, which accumulates as we collect the data as a function of reaction time.

result clearly indicate that the size of the incorporated gold nanoparticle is independent of reaction time and only the number density of nanoparticles grow with time. At the end of the reaction we have found that the wt% of gold in a typical 50 nm nanotube formed with 5.3 mM chlroauric acid solution is about 4 %. The volume percentage ϕ of gold was obtained to be 0.34 % using bulk density of gold and polypyrrole.

In Fig. 5(c) we have presented average sizes of gold nanoparticles obtained in different nanotubes as a function of concentration of chloroauric acid. The data shown here were obtained after the reaction of 60 min in different pore diameter ranging from 30 nm to 400 nm. It is clear from the Fig. 5(c) that for higher diameter nanotubes (>100 nm) the particle size is larger for higher concentration chloroauric acid solution (5.3 mM) compare to that obtained with lower concentration (2.6 mM). For the lower diameter nanotubes (<100 nm) the particle size become independent of concentration of chloroauric acid. The size of the incorporated gold nanoparticles in lower diameter nanotubes reduces slowly with the pore diameter that control diffusion and associated polymerization reaction in the nano-pores of the gold-polypyrrole composite nanotubes.

We could get systematic variation of particle size from x-ray data as the sample cell ensured that XRD data came only from these nanotubes embedded within the membrane. In Fig. 6 we have compared XRD data of a polycarbonate membrane having 200 nm diameter nanotubes of gold-polypyrrole composite (2.6 mM $HAuCl_4$) taken using the cell (shown in Fig. 2(b)) and taken in conventional transmission geometry by keeping several layers of the membrane in the x-ray beam. The XRD data was taken in transmission mode with the beam perpendicular to the surface of the membrane and that included the diffraction from the surface deposited gold nanoparticles as well. The width of the Au (111) peak (refer Fig. 6) obtained from these two types of measurements were found to be 0.58^0 and 0.24^0 respectively. The average size of particles obtained from analysis was found to be 9 nm and 22 nm respectively. The obtained value of 9 nm from the sample cell was found

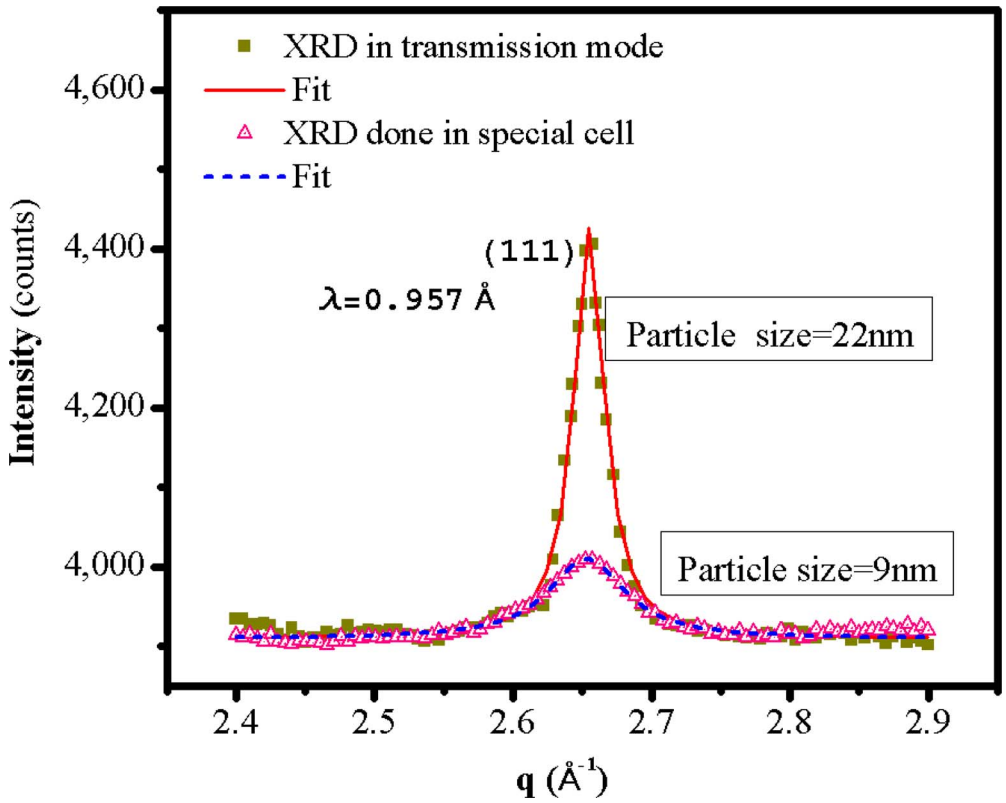

FIG. 6. The comparison of the size of gold nanoparticle of the same sample but XRD done at different configurations. The continuous line corresponds to the XRD data in transmission mode and dotted line correspond to the XRD obtained by placing the sample within sample cell, presented here.

TABLE I. The calculated values of correction factors for 200 nm, 100 nm, 80 nm and 50 nm nanotubes are shown. These factors arises due to the annular contacting area of these nanotubes with gold pad. The correction factors goes down to unity as pore density N increases.

Nominal pore diameter of membrane nanotube	Pore density obtained from SEM N($/mm^2$)	Outer diameter from TEM $d1(mm)$	Inner diameter from TEM $d2(mm)$	Correction Factor $\frac{4}{\Pi*(d1^2-d2^2)*N}$
200 nm	$4.2X10^6$	$224X10^{-6}$	$120X10^{-6}$	8.97
100 nm	$8X10^5$	$110X10^{-6}$	$60X10^{-6}$	187
80 nm	$2X10^4$	$85X10^{-6}$	$64X10^{-6}$	20389
50 nm	$2X10^4$	$50X10^{-6}$	$32X10^{-6}$	43310

to be consistent with the value obtained from TEM data shown in Fig. 2(d). This result reconfirmed that higher diameter nanoparticles are present on the surface of the membrane and we used the sample cell (shown in Fig. 2(b)) to obtain all the x-ray results presented here.

We have measured the dielectric constant of these nanotubes in the frequency range from 1 Hz to 10^6 Hz at different temperature using Novocontrol Alfa-A analyzer by depositing gold electrodes on both sides of the membranes after growth. Typical size of electrodes were 4 mm diameter that connects about 10^6 and 10^5 (refer Table I) nanotubes for membrane with pore diameter of $>$ 100 nm and $<$ 100 nm respectively. In Fig 7 inset, we have shown typical outer (d1) and inner (d2) diameter of 50 nm nanotubes. The actual connected area was obtained by using correction factors (shown in Table I). The thickness of the walls were found to be 9 nm, 10.5 nm, 25 nm, 52 nm for 50 nm, 80 nm, 100 nm, 200 nm nanotubes, respectively. The measured dielectric constants has been corrected

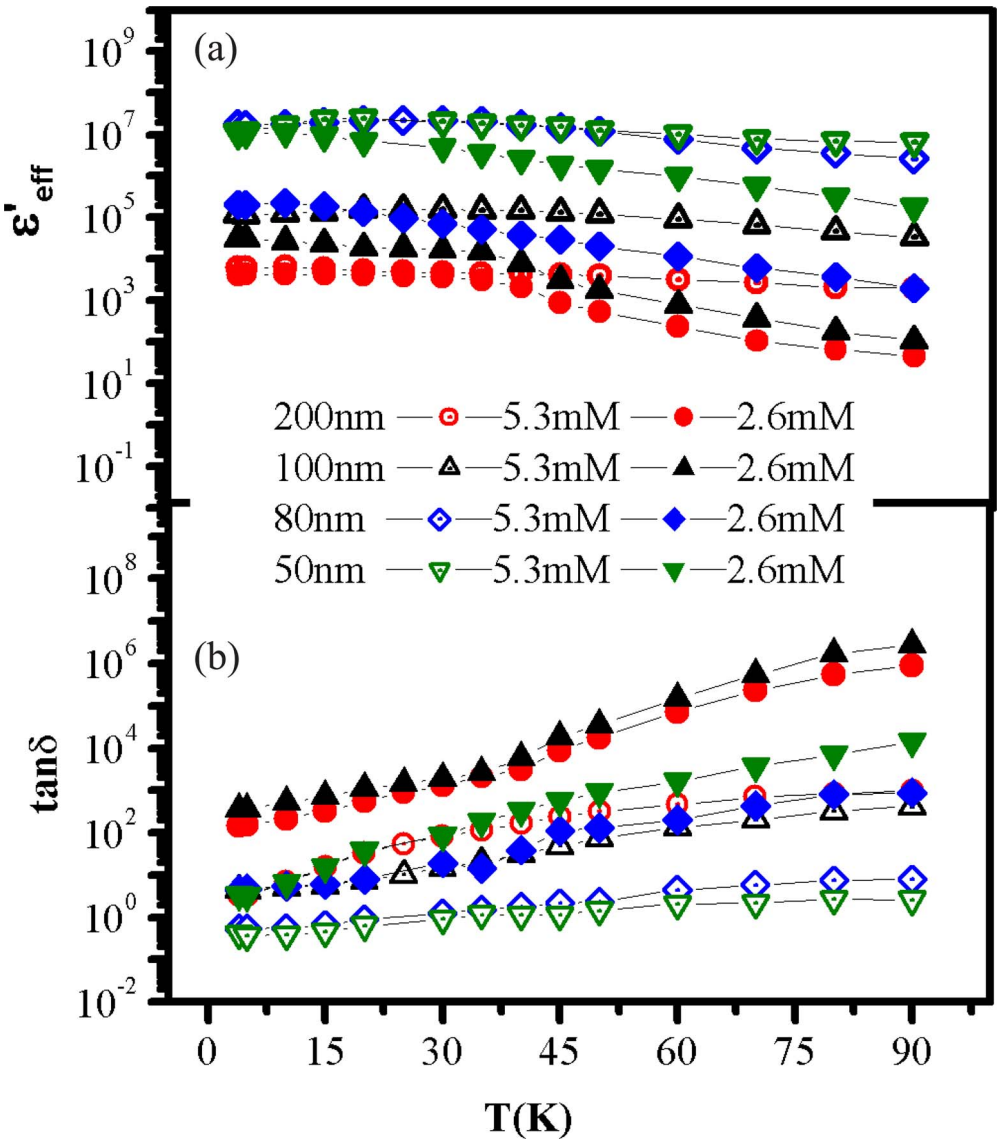

FIG. 7. (a)Temperature dependence of dielectric constant at 1kHz frequency for 50 nm, 80 nm, 100 nm, 200 nm diameter nanotubes, where empty and filled symbol correspond to 5.3 mM and 2.6 mM samples respectively, (b) dilectric loss variation for the same nanotubes are also shown.

using area of the nanotubes that connect electrodes. We have presented in Fig. 7(a) the corrected values of the real part of dielectric constant ε'_{eff} of those nanotubes as a function of temperature from 5 K to 100 K. In Fig. 7(b) we have presented the values of $tan\delta \approx \varepsilon''_{eff}/\varepsilon'_{eff}$, it is to be noted that no multiplication factors is required for $tan\delta$. In Fig. 8 we have shown both as measured (right side of figure) and corrected values (left side of figure) of ε', tanδ and σ as a function of frequency for these 50 nm diameter nanotubes. Even the measured values of real part of dielectric constant (ε') was found to be quite high (>100). However as the frequency increases the value of dielectric constant goes down and at lower temperature it starts going down at lower frequency. It is clear that dielectric constant of these nanotubes of 50 nm diameter have a colossal value of $\sim 10^7$ even above liquid nitrogen temperature (80 K) and is independent of frequency upto 1 MHz. Above 100 K the dielectric constant of the sample decays very rapidly as the CDW state in gold incorporated polypyrrole nanotube vanishes at higher temperature.[19] We have presented here results obtained with samples made using two representative Chloauric acid concentration of 5.3 mM and 2.6 mM.

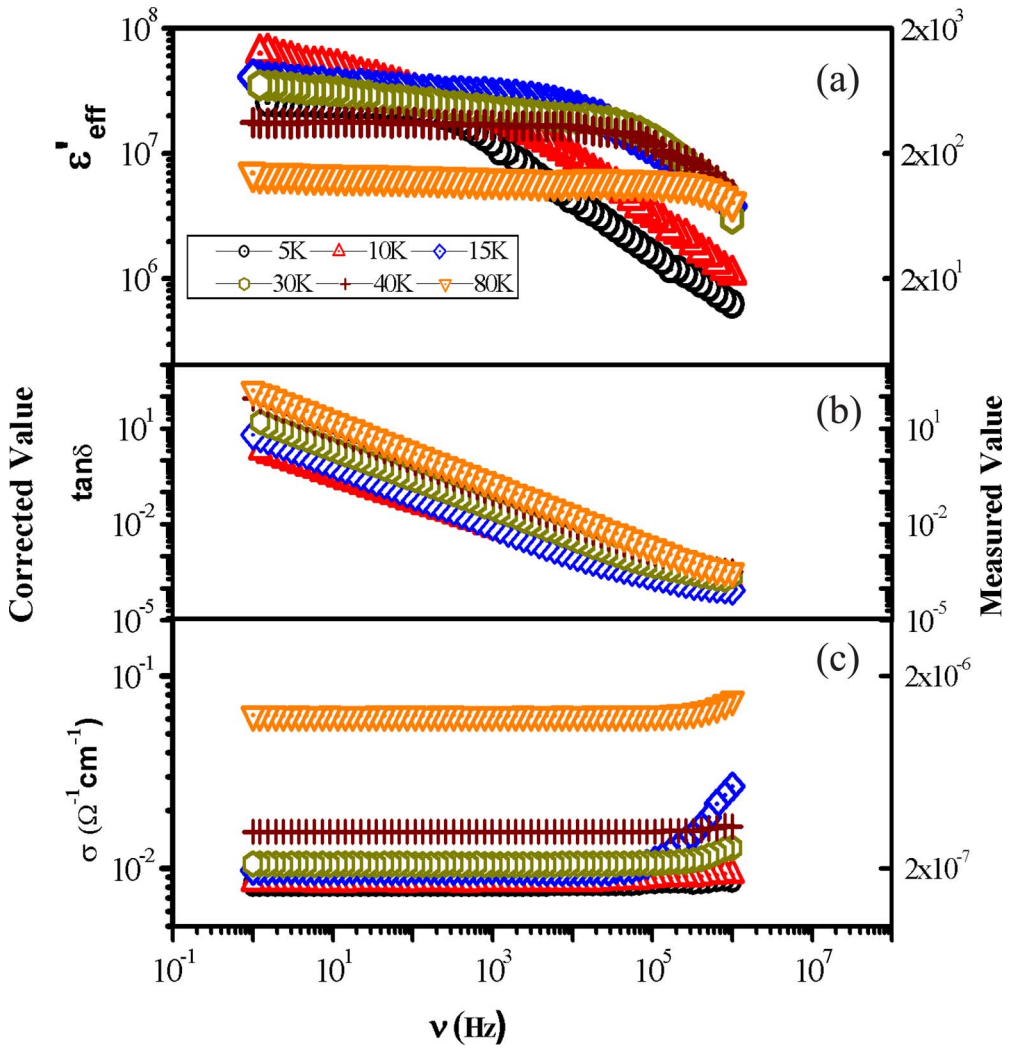

FIG. 8. Frequency dependence of (a) dielectric constant and (b) dielectric loss at different temperatures for 50 nm diameter nanotubes are shown, (c) Frequency dependence of conductivity is also shown for the same sample. Both measured values (right axis) and corrected values (left axis) are shown.

Nanotube formed with higher and lower concentration increases and reduces the volume fraction ϕ. For lower ϕ, CDW state can not survive at higher temperature as the system behave like a pure polypyrrole nanotubes.[17,18] On the other hand for higher ϕ, percolation threshold ϕ_c comes into picture. The data shown in Fig. 7 was measured at 1 kHz and it is clear that highest value of ε'_{eff} ($\sim 10^7$) was obtained for 50 nm nanotubes at both 2.6 mM and 5.3 mM concentration. However for nanotubes obtained with 5.3 mM concentration, the dielectric constant of the sample does not change much below 80 nm diameter but in case of 2.6 mM concentration the dielectric constant increases with the lowering of diameter from 80 nm to 50 nm. We found that 50 nm diameter nanotubes obtained with 5.3 mM concentration chloroauric acid, the dielectric constant is almost constant in the temperature range of 5 K to 90 K (refer in Fig. 7(b)). The obtained value of E_b for these 50 nm nanotubes was found to be 0.24 MV/m at 80 K.

IV. CONCLUSIONS

In conclusion we have studied growth processes of the gold nanoparticle incorporated polypyrrole nanotubes by in-situ x-ray diffraction technique. Our study have shown that one can obtain

colossal values of dielectric constant in these nanotubes by tuning the growth process. It is to be noted here that the colossal dielectric property presented here, required the presence of individual nanotubes to form 1D CDW state and one can increase the factors shown in Table I by increasing the number density N of pores in the membrane. Already much higher number density pores (more than 100 times) are available (SPI track-etched polycarbonate). As N increases the measured values approach the corrected values. Nearly flat frequency and temperature response of the dielectric constant of nanotubes of gold-polypyrrole composite with huge value reported here may find technological applications at liquid nitrogen temperature. Further studies are required to improve dielectric loss and E_b of these composite nanotubes for such technological applications specified by Ragone plots.[21] However with reasonable dielectric loss around 1 MHz, the composite nanotubes of 50 nm diameter prepared in polycarbonate membrane with higher pore density than reported here may already find applications as capacitor materials at liquid nitrogen temperature or lower temperature.

ACKNOWLEDGMENTS

Authors would like to thank Department of Science and technology for supporting the access of beamlines at DESY to carrying out these measurements. Authors are grateful to Dr. Stephan V. Roth (beam-line P03) and Dr. Oliver Seeck (beam-line P08) of DESY, Germany for valuable suggestions and help.

[1] Z. M. Dang, J. K. Yuan, S. H. Yao, and R. J. Liao, Adv. Mater. **25**, 6334 (2013).
[2] P. Barber, S. Balashubramanian, Y. Anguchamy, S. Gong, A. Wibowo, H. Gao, H. J. Ploehn, and H. C. Loye, Materials **2**, 1697 (2009).
[3] C. Yu, Y. S. Kim, and J. C. Grunlan, NanoLett. **8**, 4428 (2008).
[4] Y. Wang, X. Xie, and T. Goodson, NanoLett. **5**, 2379 (2005).
[5] Y. Yang, M. C. Gupta, and K. L. Dudley, Micro Nano Letts. **2**, 85 (2007).
[6] J. Huang, S. Virji, B. H. Weiller, and R. B. Kaner, Chem.-Eur. J. **10**, 1314 (2004).
[7] J. Wang, K. G. Neoh, and E. T. Kang, J. Colloid Interface Sci. **239**, 78 (2001).
[8] R. J. Tseng, J. Huang, J. Ouyang, R. B. Kaner, and Y. Yang, Nano Lett. **5**, 1077 (2005).
[9] M. Dang, J. K. Yuan, J. W. Zha, T. Zhou, S. T. Li, and G. H. Hu, Prog. Mater. Sci. **57**, 660 (2012).
[10] L. Zhang, W. Wang, X. Wang, P. Bass, and Z. Y. Cheng, Appl. Phys. Lett. **103**, 232903 (2013).
[11] S. Krohns, P. Lunkenheimer, Ch. Kant, A. V. Pronin, H. B. Brom, A. A. Nugroho, M. Diantoro, and A. Loidl, Appl.Phys.Lett. **94**, 122903 (2009).
[12] P. Monceau, Advances in Physics **61**, 2, 325 (2012).
[13] R. J. Cava, R. M. Fleming, P. Littlewood, E. A. Rietman, L. F. Schneemeyer, and R. G. Dunn, Phys. Rev. B **30**, 3228 (1984).
[14] P. Lunkenheimer, V. Bobnar, A. V. Pronin, A. I. Ritus, A. A. Volkov, and A. Loidl, Phys. Rev. B **66**, 052105 (2002).
[15] P. B. Littlewood, Phys. Rev. B **36**, 3108 (1987).
[16] A. Rahman and M. K. Sanyal, Adv. Mater. **19**, 3956 (2007).
[17] A. Rahman and M. K. Sanyal, Phys. Rev. B **76**, 045110 (2007).
[18] A. Rahman and M. K. Sanyal, ACS Nano. **7**, 7894 (2013).
[19] A. Sarma, M. K. Sanyal, A. Rahman, and B. Satpati, J. Appl. Phys. **112**, 044304 (2012).
[20] I. Sarkar, A. Sarma, M. K. Sanyal, S. Thieß, and W. Drube, J. Appl.Phys. **114**, 163707 (2013).
[21] T. Christen and M. W. Carlen, Journal of Power Sources **91**, 210 (2000).
[22] M. K. Sanyal, V. V. Agrawal, M. K. Bera, K. P. Kalyanikutty, J. Daillant, C. Blot, S. Kubowicz, O. Konovalov, and C. N. Rao, J. Phys. Chem. C **112**, 1739 (2008).
[23] G. K. Williamson and W. H. Hall, Acta Metall. **1**, 22–31 (1953).
[24] S. V. Roth, H. Walter, M. Burghammer, C. Riekel, B. Lengeler, C. Schroer, M. Kuhlmann, T. Walther, A. Sehrbrock, R. Domnick, and P. Müller-Buschbaum, Appl. Phys. Lett. **88**, 021910 (2006).
[25] O. H. Seeck, C. Deiter, K. Plaum, F. Bertam, A. Beerlink, H. Franz, J. Horboch, H. Schulte-Schrepping, B. M. Murphy, M. Greve, and O. Magnussen, J. Synchrotron Radiat. **19**, 30 (2012).
[26] M. Sharma, M. K. Sanyal, B. Satpati, O. H. Seeck, and S. K. Ray, Phys. Rev. B **89**, 205304 (2014).